JOURNAL OF MATERIALS SCIENCE 31 (1996) 1183–1197

Influence of reprocessing on properties of short fibre-reinforced polycarbonate

A. CHRYSOSTOMOU, S. HASHEMI
School of Polymer Technology, University of North London, Holloway Road, London N7 8DB UK

The influence of reprocessing by injection moulding on properties of polycarbonate has been studied. It was found that reprocessing reduces the mean fibre length and increases the melt flow index. There was no variation in tensile or flexural properties with the number of reprocessing cycles. Fracture toughness, K_c, measured via notched tensile and flexural bars indicated that the material toughness is affected by the number of reprocessing cycles. The effect was more pronounced in bending than in tension. Strain energy release rate, G_c, was found not to be affected significantly by the number of reprocessing cycles. Although, as the material was reprocessed, fracture parameters were always lower than that of the virgin unprocessed material.

The influence of reprocessing on weld-line properties was also investigated using notched tensile specimens. It was found that whereas tensile strength is not affected by the presence of the weld-line, fracture toughness deteriorated significantly, giving a weld-line integrity factor, F, of 0.75. The value of F was not affected significantly by the number of reprocessing cycles.

1. Introduction

In recent years the practice of recycling has been encouraged and promoted with the increased awareness in environmental matters and the subsequent desire to save resources. This together with the relatively high cost of the polymer and some times high levels of scrap material generated during manufacture, make this procedure both a viable and attractive option. However, with the high temperature and pressure utilised during processing, the material is subjected to conditions which would cause detrimental effects to the polymer in terms of properties.

Several papers [1–3] have been published concerning the effect of recycling on molecular weight and some important mechanical properties such as tensile strength, flexural modulus and impact strength of polycarbonate material. However, because of the ever increasing use of polycarbonate as matrix for composite materials, it is important to establish how these properties are affected when fibre-reinforced polycarbonate material is reprocessed. In view of this, a grade of polycarbonate containing 20% by weight short fibres was initially injection moulded in the present work in order to establish the characteristics of the virgin material. This was then used to gauge the effects arising from reprocessing and regrinding of the virgin material during five recycling processes. Quantities measured include, the melt flow index, the tensile and flexural strengths, the elastic modulus and the fracture toughness. Moreover, since most injection moulding components contain a weld-line of one type or another, it was of interest also to examine the effects that reprocessing may have on mechanical properties of welded components.

2. Experimental procedures

2.1. Material

Materials used in this study were received courtesy of BAYER UK. The product is known commercially as Makrolon 8025 which is a grade of polycarbonate (PC) reinforced with 20% by weight (w/w) short glass fibres. The material was dried prior to all processing cycles according to the manufacturer's recommendations, i.e. for a minimum of four hours at 120 °C. Moreover, it was found that in order to overcome problems of drool the material had to be exposed to elevated temperatures overnight.

2.2. Mouldings

Three types of specimens were injection moulded as shown in Fig. 1;

(i) *Tensile bars*: dumbbell shaped tensile specimens of dimensions 1.7 × 12.5 × 125 mm were produced on a Negri Bossi NB60 with the melt temperature set at 320 °C and a mould temperature set at 80 °C. Injection speeds reached 208 rpm while the pressures were held at 70 bar. The mould used consisted of two cavities, a single feed and a double-feed cavity as shown in Fig. 1. In the latter, a weld-line is formed as two opposing melt fronts meet at the centre.

0022–2461

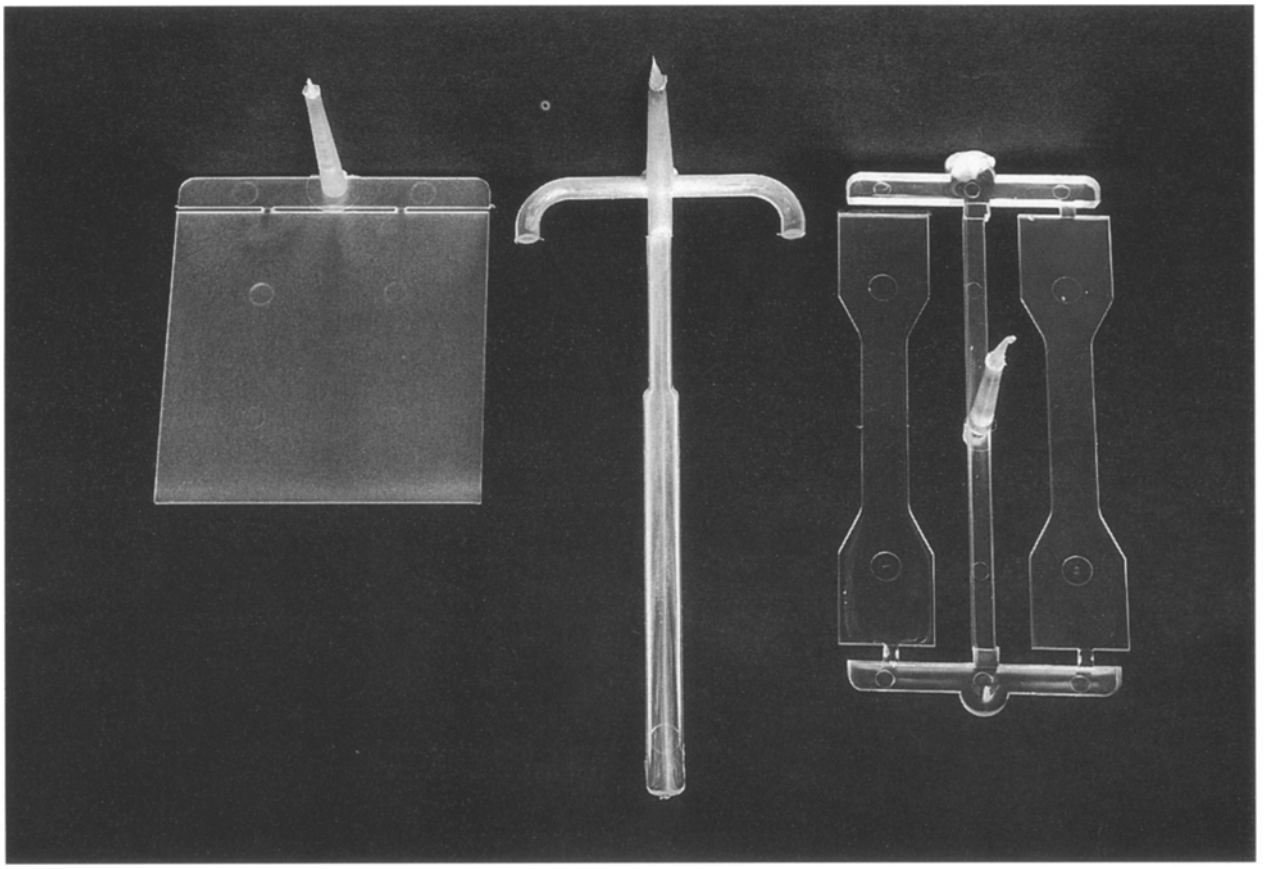

Figure 1 Injection mouldings used; tensile bars, flexural bars and plaque mouldings.

(ii) *Flexural bars*: flexural specimens were produced on a Szekely Hydrojet injection moulding machine using an edge gated rectangular cavity of dimensions $4 \times 10 \times 120$ mm as shown in Fig. 1. The processing temperature was set at 290 °C and the mould temperature was set at 40 °C with a pressure of 54 bar.

(iii) *Plaques*: Square plaques of dimensions $88 \times 88 \times 1.5$ mm were produced on a Peco 15MR injection moulding machine fitted with a single mould cavity. The cavity was filled by the molten material either through an edge-gate or a double-edge-gate as shown in Fig. 1. In the latter, a weld line is formed as two adjacent flow fronts meet. Plaques were processed at a melt temperature of 330 °C and a mould temperature of 80 °C with pressures attaining 114 bar.

2.3. Reprocessing

The material was received in the form of granules and was at first, injection moulded to produce the above mouldings. These mouldings are referred to in the following text as virgin or zero cycle. After testing the virgin test pieces, they were then granulated on a Blackfriars 2000 granulator and remoulded (reprocessed) again to produce the first recycled test pieces. The regrinding and remoulding procedures were carried out five times, maintaining the processing conditions as closely as possible to those which were used for the original material (i.e. that of the virgin material as described above). Each subsequent cycle after the zero cycle, was referred to as; first cycle, second cycle, and so forth, up to and including the fifth cycle.

3. Results and discussion

3.1. Fibre length distribution

The measurement of the length of the reinforcing fibre was carried out by burning off the organic polymer matrix in a muffle furnace. At 650 °C glass undergoes devitrification and although there is no weight loss, the fibre will become brittle and readily breaks, thus exaggerating the degree of degradation. For this reason the furnace temperature was maintained at 600 °C. The chard remaining in the muffle was then viewed under an optical microscope. A series of photographs were then taken as shown in Fig. 2 from which some 500 fibre lengths were counted. When the counting was completed a frequency distribution of fibre lengths was plotted for each material as shown in Fig. 3(a–d). The mean and median fibre lengths as derived from these plots are delineated in Table I. It can be seen that during reprocessing–regrinding procedures, the glass fibre is severely degraded. Even in the absence of any regrinding as for the virgin material, the glass fibre is degraded during injection process alone. The mean fibre lengths for the reprocessed materials relative to that of the unprocessed granules are plotted in Fig. 4 as a function of reprocessing cycles. As can be seen the ratio is fairly constant up to second recycle after which it drops sharply before reaching a constant ratio of 0.64.

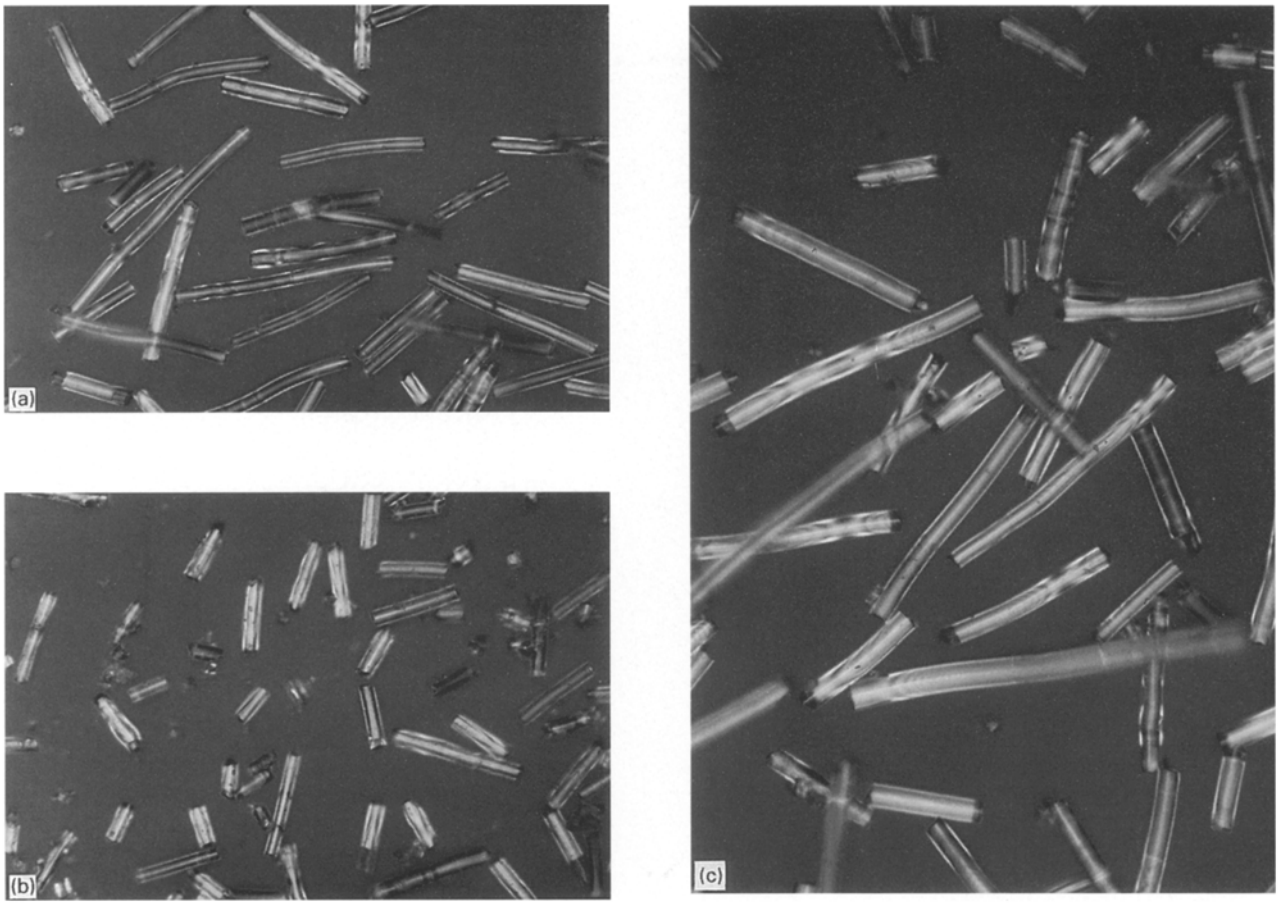

Figure 2 Micrographs showing fibre lengths for; (a) granules, (b) virgin and (c) after fifth cycle.

3.2. Melt flow index (MFI)

The melt flow index of Makrolon 8025 was measured after each reprocessing cycle using a Davenport Rheometer. Measurements were carried out as specified by ASTM D1238, i.e. at 300 °C and with a 1.2 kg load.

After repeated moulding cycles, the translucent and colourless PC composite showed progressive darkening but the translucency was maintained. This result is a first indication that some form of degradation–decomposition occurs during the moulding operation due to the high temperatures used.

Fig. 5 shows the plot of the MFI as a function of reprocessing cycles, where each data point represents an average value taken from at least four measurements. As can be seen, the MFI increases continuously with the number of reprocessing cycles. An even faster increase is observed from the second cycle onwards. The MFI is approximately three times higher than that of the original value after five cycles. It is interesting to note that this increase in MFI is consistent with the results of Eguiazabal and Nazabal [1]; these workers observed an increase in the MFI during reprocessing of the unreinforced polycarbonate material. This increase in the fluidity of the reprocessed material is partly due to the shortening of fibres as a result of reprocessing and regrinding cycles and partly due to the decrease in molecular weight of the polymer arising from the reduction in polymeric chain lengths by degradation mechanisms [1] during repeated processing.

3.3. Infrared (IR) Analyses

The infrared (IR) analyses were performed in a Perkin Elmer 1600 FTIR spectrophotometer. Samples taken from each reprocessing cycle were dispersed on a diamond coated disc. The disc was then placed in an infrared spectrophotometer and the resulting spectrograph was printed.

Fig. 6 shows an example of the FTIR traces obtained for the virgin and the fifth recycled material. Evidently, there are no changes in the spectra; thus indicating that under the present processing conditions, degradation reactions caused a decrease in the molecular weight but did not affect the intrinsic chemical structure of the polymer.

3.4. Tensile tests

Tensile tests were carried out on the dumbbell shaped specimens with and without weld-lines in an Instron testing machine at room temperature and at a crosshead displacement rate of 5 mm min^{-1}. The quantities measured from the recorded load–displacement diagrams (see Fig. 7) for all the materials were: (i) the nominal tensile yield stress calculated on the basis of the maximum load and (ii) the nominal stress at a break. The average value of these quantities and their standard deviations are given in Table II. A minimum of eight specimens were tested for each material.

The broken unwelded test pieces are shown in Fig. 8 and as can be seen they have been broken after some

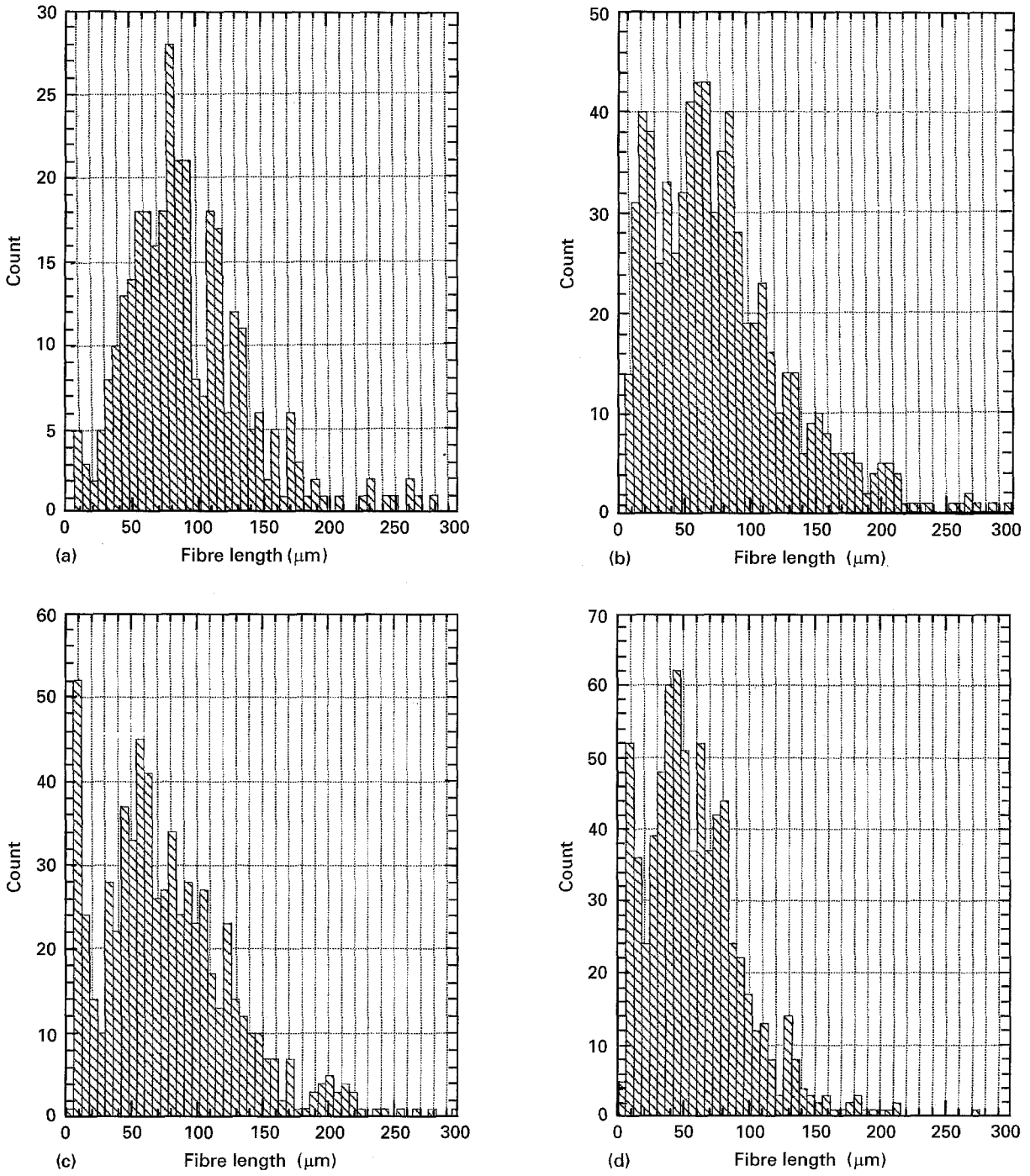

Figure 3 Fibre length histograms; (a) granules, (b) virgin, (c) after 2nd cycle and (d) after fifth cycle.

TABLE I Fibre length studies (μm)

N_r	Mean	Median	Number
Granules	92	84	312
Virgin	79	70	704
2nd	78	70	650
3rd	62	50	607
4th	59	49	506
5th	59	52	736

degree of plastic deformation. The values given in Table II indicate that the tensile yield and breaking strengths show no systematic variation with the number of reprocessing cycles.

The dumbbell test pieces that contained a weld-line all broke at this line. The comparison between the weld and unwelded tensile data is shown in Table II through a "weld-line integrity" parameter, F, defined as the strength of the weld-line specimen divided by the strength of the weld-free specimen. Using this parameter, a ratio of unity represents weld-line insensitivity and the lower values represent degrees of vulnerability. As can be seen the weld-line integrity parameter for the tensile yield stress or the breaking stress is very close to unity and in some cases marginally higher, therefore, indicating that the quantities measured did not deteriorate significantly in the presence of the weld-lines, regardless of the number of reprocessing cycles.

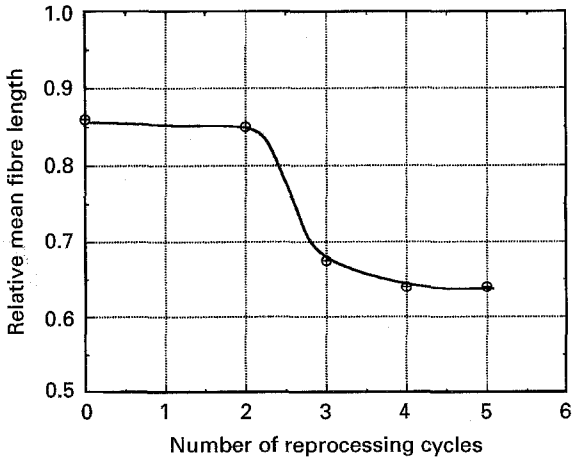

Figure 4 Relative fibre length versus the number of reprocessing cycles.

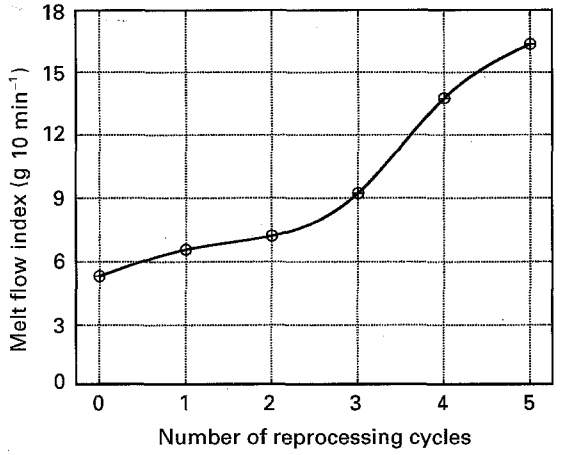

Figure 5 Melt flow index over a period of 10 min versus the number of reprocessing cycles.

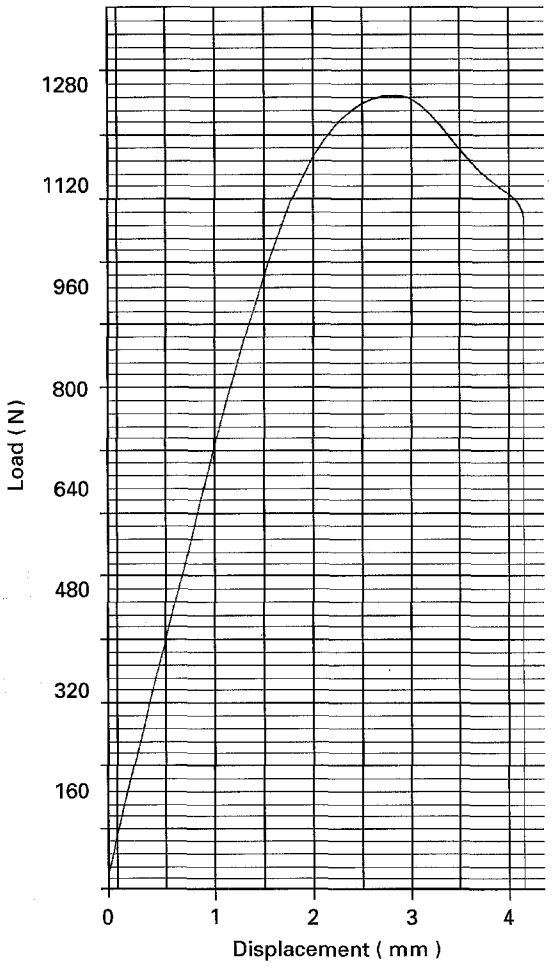

Figure 7 A typical tensile load–displacement diagram taken on a virgin specimen.

3.5. Flexural tests

The three point bend flexural modulus and strength as a function of reprocessing cycle were determined by testing the flexure bars (thickness of 10 mm and depth of 4 mm) at a crosshead displacement rate of 5 mm min^{-1} with span to depth ratio of 20:1. The flexural load–displacement diagrams obtained for these materials were similar to those obtained from tensile tests. Linear elastic behaviour was observed at first, which became exceedingly non-linear as the maximum load was reached. Because of this, flexural strength values were computed using the plastic collapse equation which gives strength values which are 1.5 times lower than that predicted by the linear elastic equation. Flexural modulus values were calculated from the initial linear part of the load–displacement diagrams. Results obtained are presented in Table III, where each value represents an average of eight measurements. The quantities measured show very little change, if any, with the number of reprocessing cycles. The flexural modulus of the recycled materials

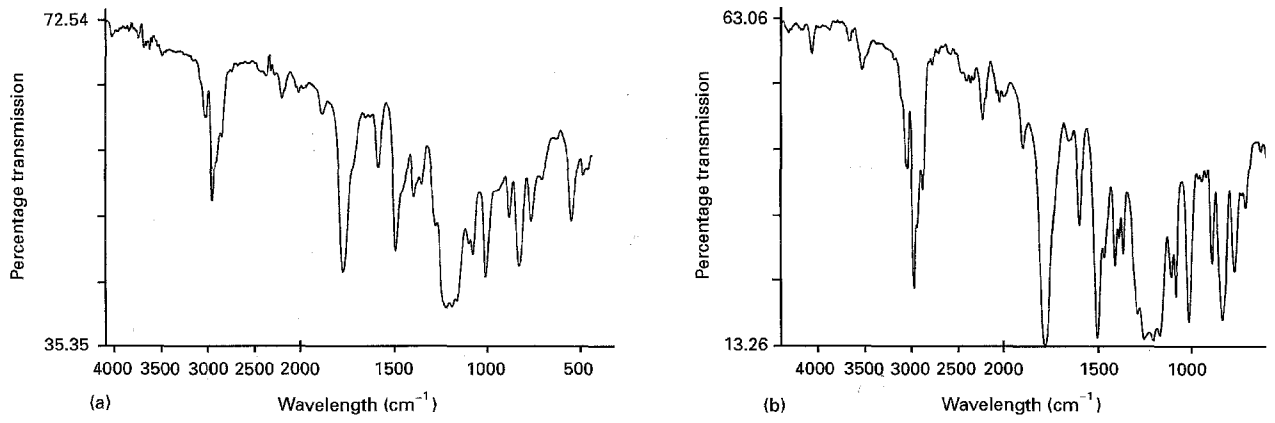

Figure 6 Infra-red spectra for (a) the virgin and (b) the fifth recycled materials.

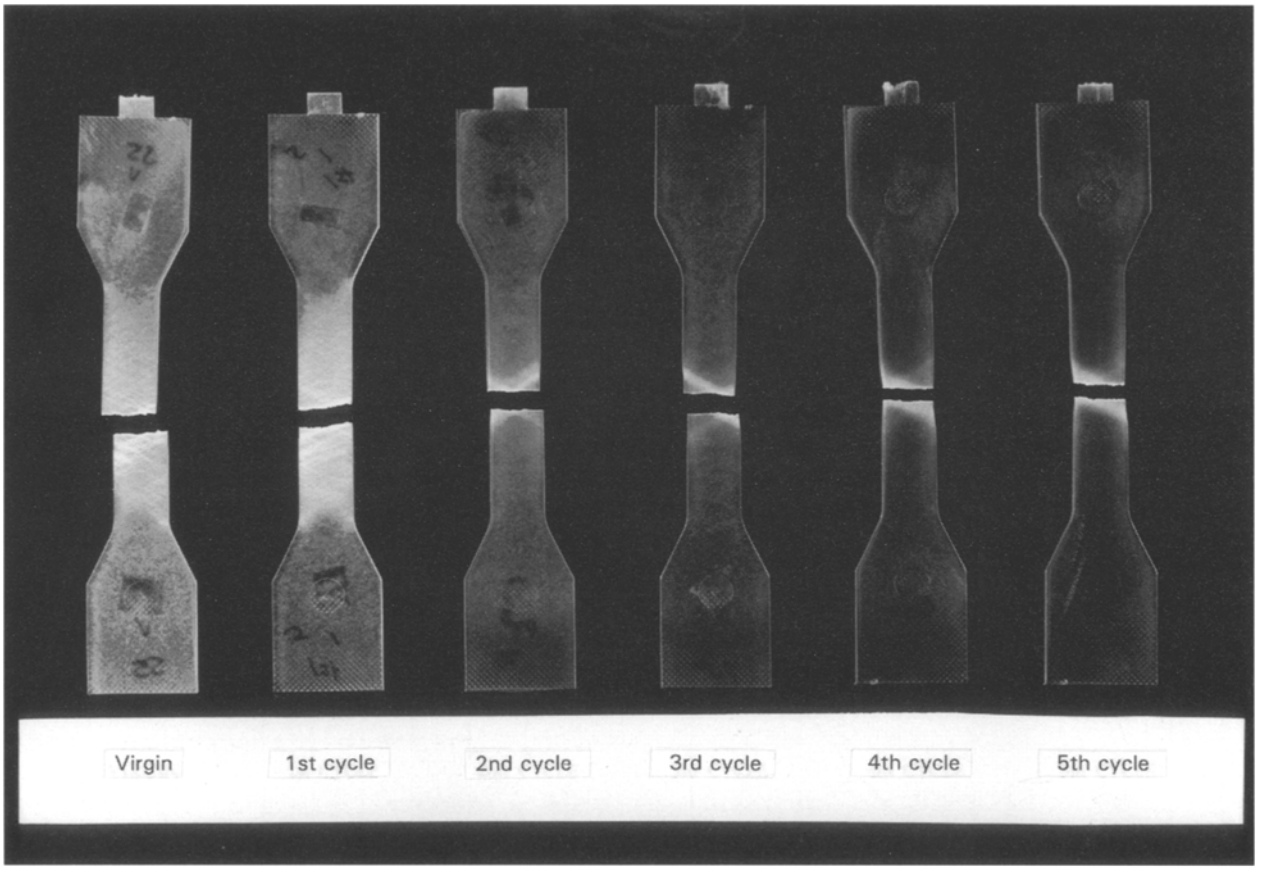

Figure 8 Broken tensile test bars for the virgin and the reprocessed materials.

TABLE II Tensile properties

N_r		σ_y [MPa]	F	σ_b [MPa]	F
0	unwelded	62.17 [2.47]	1.04	54.54 [3.90]	1.01
	welded	64.53 [0.271]		54.98 [4.05]	
1		59.59 [1.52]	1.04	52.06 [0.50]	1.05
		61.70 [0.780]		54.59 [2.66]	
2		64.25 [0.90]	0.98	53.25 [1.84]	1.03
		62.87 [0.58]		54.89 [5.10]	
3		63.32 [0.17]	0.99	52.03 [0.46]	1.01
		62.70 [0.23]		52.27 [0.69]	
4		64.32 [1.26]	0.96	54.36 [2.24]	0.99
		62.00 [1.13]		53.98 [2.14]	
5		63.55 [2.10]	0.99	54.31 [0.56]	1.00
		62.89 [1.18]		54.35 [1.71]	

Note: σ_y = yield stress, σ_b = breaking stress

TABLE III Flexural properties

N_r	σ_y [MPa]	E_f [GPa]
0	171.3 [1.47]	3.24 [0.07]
1	166.9 [5.35]	3.03 [0.16]
2	164.7 [2.09]	3.00 [0.13]
3	166.1 [1.12]	3.06 [0.06]
4	169.8 [1.93]	3.07 [0.10]
5	166.7 [3.88]	2.90 [0.04]

remains effectively constant at 3 GPa, which is approximately 8% lower than that of the virgin material, whereas the flexural strengths of the virgin and the reprocessed materials showed insignificant differences.

3.6. Notched impact strength

The notched impact strength of the virgin and the reprocessed material was measured using three point bend Charpy impact specimens of thickness, B, and depth, D, of 4 and 10 mm respectively. Specimens were notched to an a/D ratio of 0.3 using a V-shaped cutter with a tip radius of 0.25 mm and fractured at the pendulum speed of 3 $m\,s^{-1}$ at room temperature. The influence of the number of reprocessing cycle on the impact strength is shown in Fig. 9, where each datum represents the average of ten measurements. All the specimens fractured in a brittle manner, and as can be seen, a clear decrease in impact strength is observed with number of reprocessing cycles, with the fifth recycled material exhibiting a drop in impact strength of about 16% compared to that of the virgin material.

3.7. Tensile testing of notched bars

The fracture testing of the notched tensile bars was performed on rectangular coupons (prepared from the plaque mouldings) with a length of 90 mm and a width of 20 mm. Single edge notched tension (SENT) specimens were prepared from the weld and unwelded plaques with their length either parallel or perpendicular

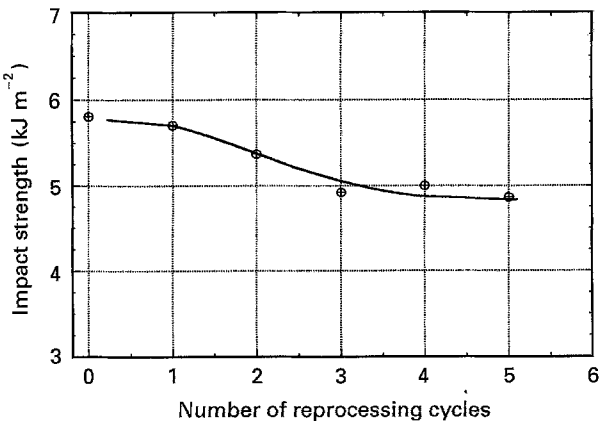

Figure 9 Impact strength versus the number of reprocessing cycles.

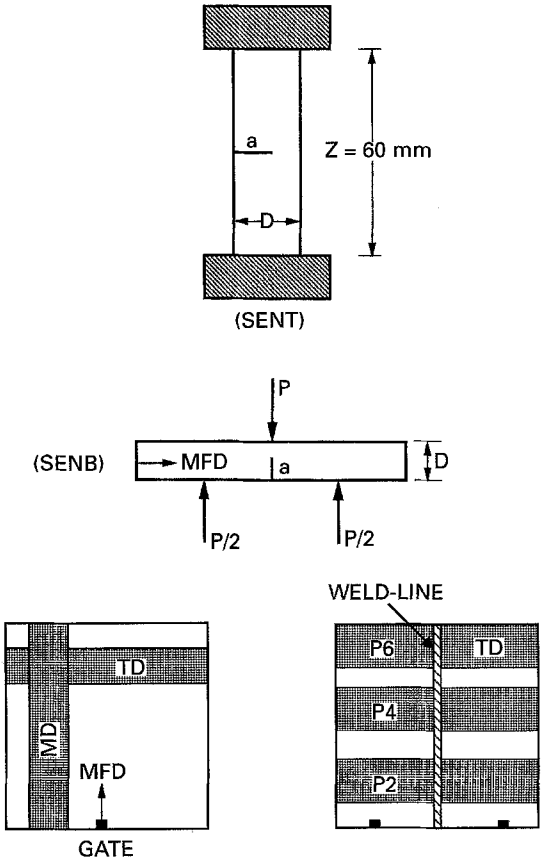

Figure 10 Specimen configurations for fracture toughness determination.

to the melt flow direction (MFD) as shown in Fig. 10. These different specimen orientations relative to MFD are referred to as flow direction (MD) and the transverse direction (TD) respectively in the following text. The initial notch thus ran either perpendicular or parallel to the MFD. Single edge notches were then inserted half way along the length of the specimens (see Fig. 10) with the length of the edge notch varying from 0.1D and 0.7D. In the case of specimens with a weld-line (formed by two opposing flow fronts as in dumbbell specimens or two parallel fronts as in plaque mouldings), the initial notch was inserted inside the weld-line. These single-edge notched bars were tested in tension in an Instron testing machine using pneumatic grips with gauge length, z, of 60 mm. The notches were inserted by first forming a saw cut which was then sharpened using a razor blade with a tip of radius of approximately 6 μm. Subsequent to fracture, the notch depth, a, of each specimen was measured using a travelling microscope.

Additionally, the strength of the unnotched coupons was also measured. Although, this type of measurement was already performed on the virgin and reprocessed materials (see Table II), it has been reported that such a measurement is dependent upon the thickness of the moulding and the manner in which the mould is filled. Indeed, the strength results obtained from the unnotched coupons cut from the square plaques averaged about 52 MPa which is approximately 20% lower than those obtained by way of dumbbell shaped specimens. The unnotched strength values were obtained on 10 mm wide rather than 20 mm wide specimens to avoid slippage from the grips before fracturing.

3.8. Crack growth behaviour

In all cases the initial crack propagated perpendicular to the direction of the applied load and the manner in which the specimens fractured was not significantly affected by the number of reprocessing cycles or by the presence of the weld-line in the specimens. Typical load–displacement records obtained from the notched tensile specimens are shown in Fig. 11(a). The nature of these curves and many others obtained in the present study suggests some amount of slow crack growth (or damage at the crack tip) occurs before the onset of unstable fracture. The load–displacement traces were all initially linear but deviated from linearity as slow crack growth or damage occurred in the vicinity of the crack tip before the maximum load was reached. The growth of the crack and the damage zone was collinear with the original notch. Prior to complete fracture of test pieces the following observations were made:

(i) Development of a damaged zone in the form of stress whitened region at the tip of the crack, at a load below that required for fracture (see Fig. 11(b)). Generally, the load at which the damage zone was first observed corresponded closely to the point at which non linearity had commenced in the load–displacement diagram. This observation was consistent regardless of the number of reprocessing cycles.

(ii) The damage zone was seen to grow from the tip of the crack normal to the direction of the applied stress under rising load. At the maximum load, the damage zone was extended over a large proportion of the sample width hence weakening the ligament area and suppressing further increase in the applied load. At this point the initial notch propagated rapidly through the damage zone, or as in some cases, slowly tearing through it (see Fig. 11(a)). It must be noted that there was always some amount of slow crack growth prior to the attainment of maximum load suggesting that the initial crack had propagated before the maximum load was reached. The amounts which the initial crack extended prior to reaching the maximum load was always less than 1 mm.

3.9. Fracture of the specimens without a weld-line

The fracture behaviour of the virgin and several of the reprocessed materials is presented in Fig. 12(a, b). In this figure, the failure stresses, σ_f, were determined from maximum loads and plotted against the relative crack length a/D. Fig. 12(a, b) represents the behaviour for the MD and TD directions respectively. Fig. 12(a, b) shows that the fracture stress decreases with increasing a/D. Evidently, specimens having initial cracks which are normal to the melt flow direction (MD) fracture at lower stresses than TD specimens in which the initial cracks run parallel to the melt flow direction. In each case, the virgin material fractured at relatively higher stresses than the reprocessed materials. For comparison, each figure is superimposed by plots determined by applying the notch-insensitive analysis; where the notch-insensitive fracture stress (net-section stress), σ_N, is related to the length of the crack, a, by the relationship;

$$\sigma_N = \sigma_y \left(1 - \frac{a}{D}\right)^2 \quad (1)$$

where σ_y is the tensile yield stress of the unnotched specimen. Clearly, the fracture stress for the middle range crack lengths is well below that required for the net-section to yield; whereas for long and short crack lengths it is at close proximity to the net-section yielding line.

Fracture toughness (K_c) was obtained through the analysis of single-edge notched (SEN) tensile tests, where the critical value of stress field intensity factor (fracture toughness) is determined from the expression [4]:

$$K_c = \sigma_f Y a^{1/2} \quad (2)$$

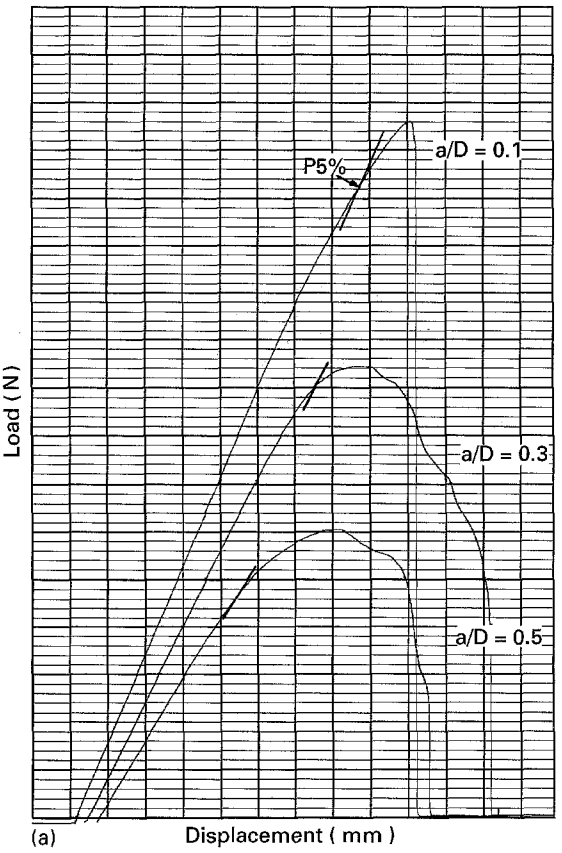

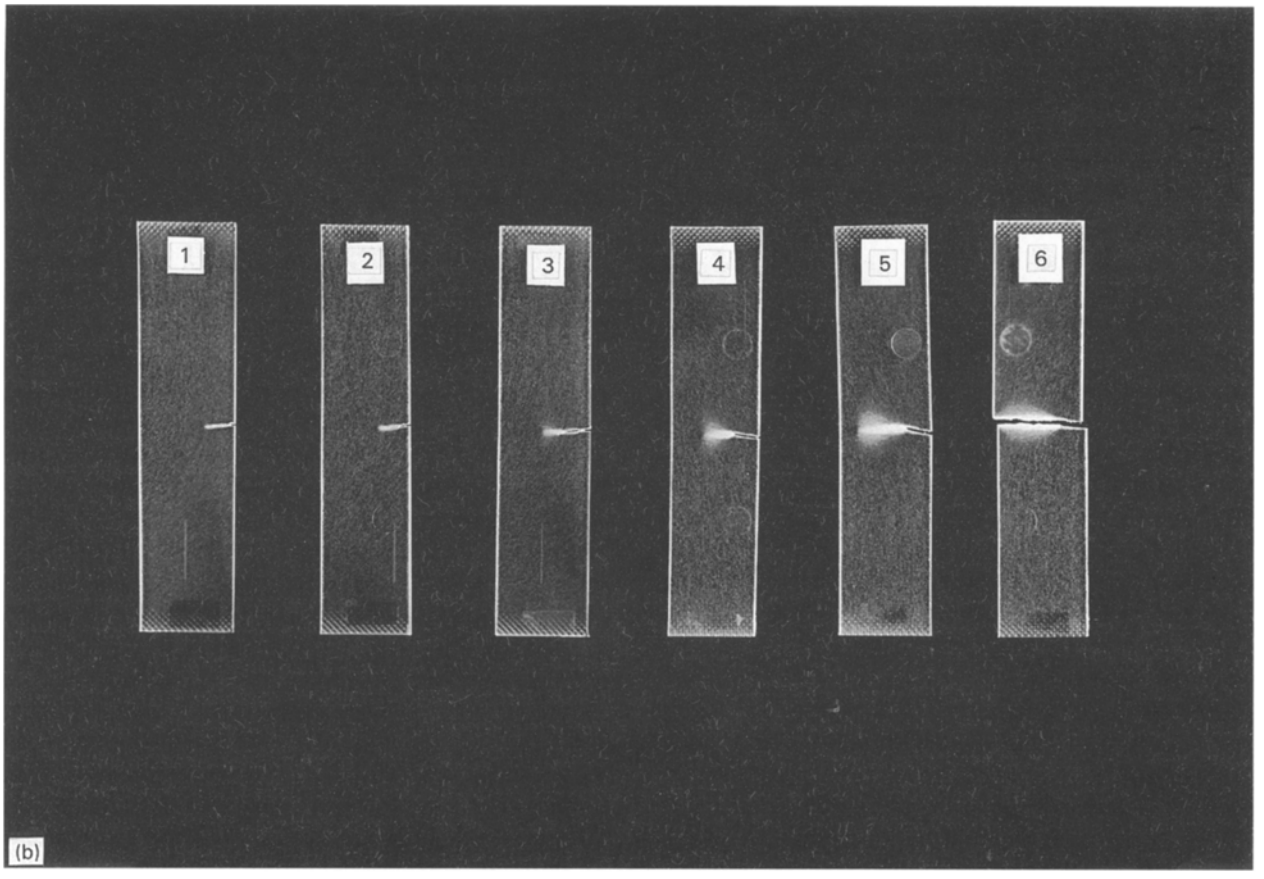

Figure 11 (a) Typical load–displacement diagrams for several a/D ratios. P5% is also indicated. (b) SENT fractured specimens showing the damage zone at the tip of the crack.

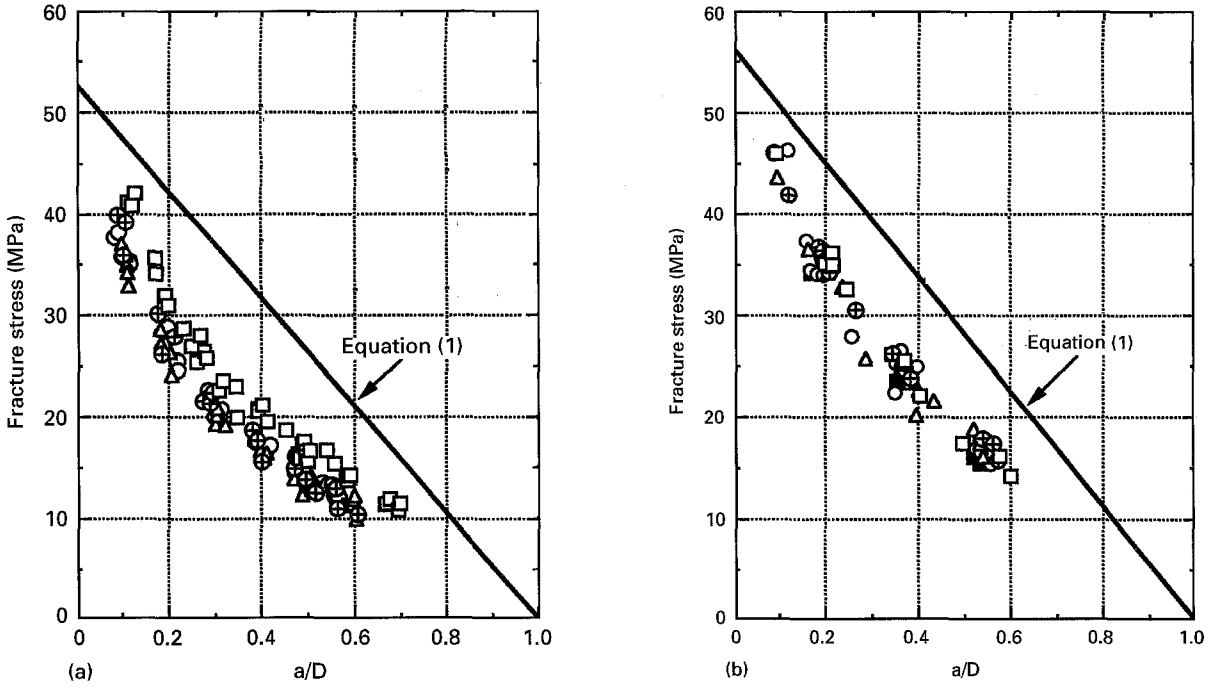

Figure 12 Fracture stress for SENT specimens versus relative crack length for the virgin and the reprocessed materials; (a) MD specimens, □ virgin, ⊕ 1st cycle, △ 2nd cycle, ○ 3rd cycle, ■ 5th cycle and (b) TD specimens, with the symbols retaining their previous meanings.

where σ_f is the far field fracture stress, a is crack length and Y is the finite width correction factor. Since the notched tensile specimens were simply clamped in the Instron machine, the expression of the geometry factor, Y, given by Brown and Srawley [4] is inappropriate. It assumes that the tensile force is uniformly distributed across the width of the specimen which is consistent with pin-loading. For our present loading configuration, a more appropriate expression is [5]:

$$Y = \frac{5\pi^{1/2}}{(20 - 13x - 7x^2)^{1/2}} \quad (3)$$

where $x = a/D$. The variation of Y with x is shown in Fig. 13 and compared with the commonly used Brown–Srawley calibration function. It is apparent that when the specimen is clamped the Y function varies less with x as compared to the situation in which the specimen is pin-loaded.

Fig. 14(a, b) shows σ_f plotted against $[Ya^{1/2}]^{-1}$ (unit of $m^{-1/2}$) for the virgin and three of reprocessed materials for both MD and TD directions. From these plots the following observations can be made: the variation of σ_f with $[Ya^{1/2}]^{-1}$ is fairly linear for crack lengths bigger than 0.1D, thus indicating that the fracture toughness, K_c, is independent of the crack length; TD specimens exhibit higher slopes hence higher fracture toughnesses than MD specimens. Fracture toughnesses and 95% confidence limits are delineated in Table IV. These values indicate that K_c is not significantly affected by the number of reprocessing cycles, although once the material is reprocessed, it exhibits relatively lower fracture toughness than the virgin material. Furthermore, it is clear that K_c values in the TD direction are consistently higher than corresponding values in the MD direction; the

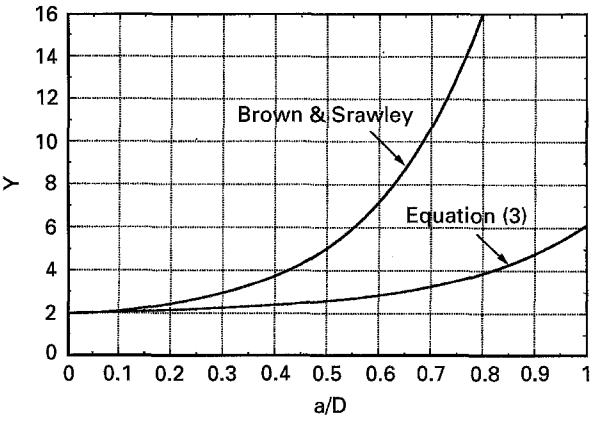

Figure 13 Variation of Y with relative crack length for pin-loaded and clamped specimens.

ratio gives some indication about the degree of anisotropy which apparently is not affected significantly by the number of reprocessing cycles.

It should be appreciated from a technical point of view, that the results obtained appear to be satisfactory; in the sense that over a wide range of a/D, K_c values do not depend upon the initial length of the crack and that the variation in the results is no greater than that observed in fracture toughness tests. Therefore it would appear that present K_c values are useful, as a first approximation, for comparing the material response to crack propagation as a function of reprocessing cycles. The size of the damage zone and that of the specimen could modify the result; in a similar manner to that in which the size of plastic zone can affect metals or unreinforced plastic materials. However, the main difference between the damaged zone at the notch tip and the plastic zone is that whereas the latter opposes the rapid propagation of

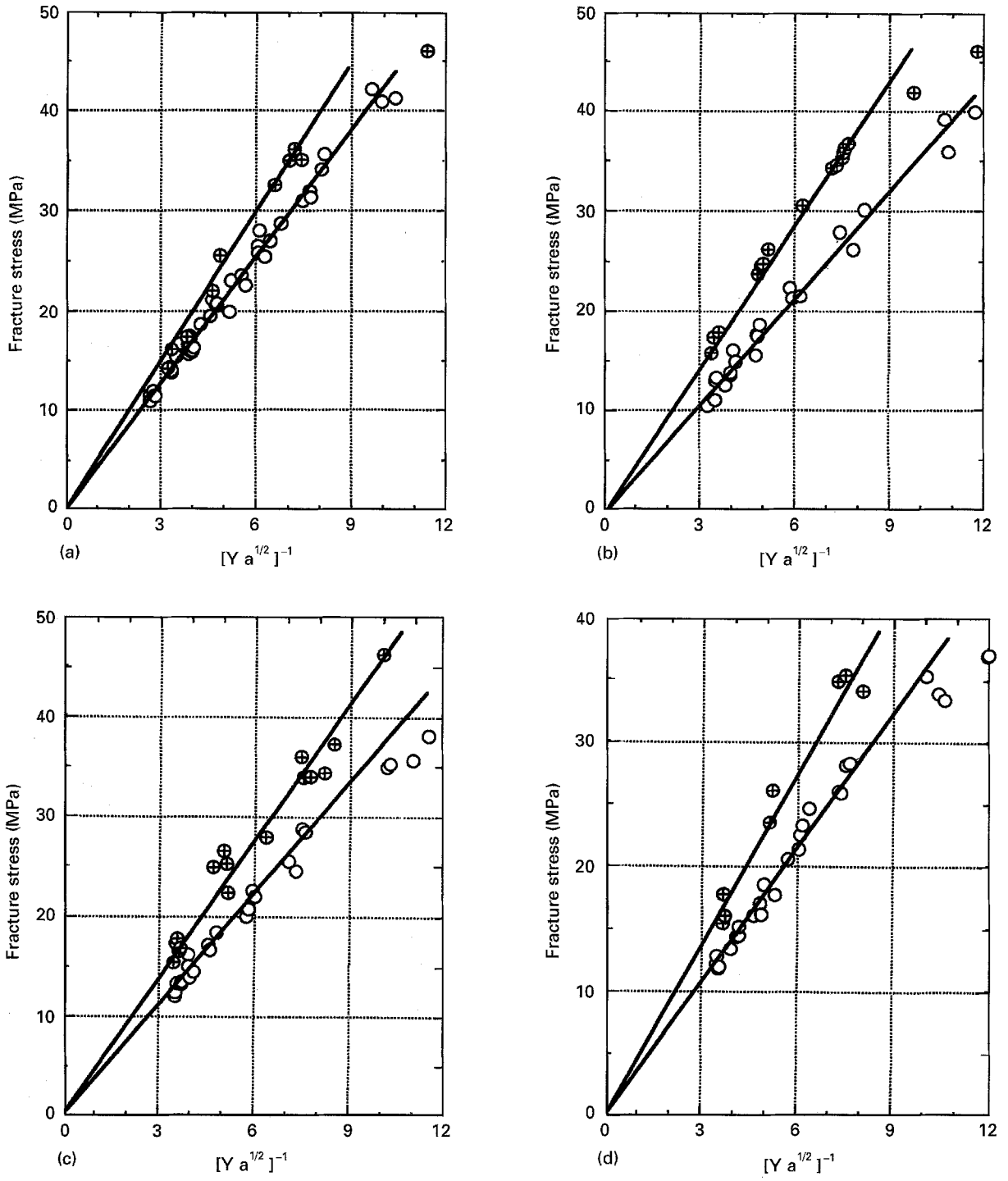

Figure 14 Fracture stress (⊕ TD, ○ MD) for SENT specimens versus $[Ya^{1/2}]^{-1}$ for (a) the virgin material and (b–d) the re-processed material after 1, 3 and 5 cycles respectively.

TABLE IV Fracture toughness, K_c [MPa m$^{1/2}$]

N_f	K_c, MD	K_c, TD	(K_c, TD)/K_c, MD)
0	4.23 ± 0.05	4.90 ± 0.16	1.16
1	3.56 ± 0.08	4.82 ± 0.06	1.35
2	3.51 ± 0.07	4.69 ± 0.12	1.34
3	3.66 ± 0.08	4.60 ± 0.15	1.26
4	3.52 ± 0.05	4.50 ± 0.17	1.28
5	3.61 ± 0.07	4.62 ± 0.25	1.28

the crack and delays breakage, the former constitutes the normal process of crack propagation whereby the material is weakened; this weakening is a contributing factor in assessing breakage. In general, when attempting to define a K_c for a material which does not conform to classical brittle fracture, the terms fracture stress and the crack length in Equation (1) each poses a question. Should fracture stress be calculated from the maximum load or from the candidate fracture load, P_q, obtained by a 5% change in slope of the linear portion of the load–displacement diagram [4]; and should crack length be taken as the initial notch depth, or an effective crack length corresponding to maximum load? Regarding the first question, although in some composites one may argue that determining K_c from P_q is justified, for the materials studied here, because considerable damage preceded fracture; the 5% P_q approach which allows only 1–2 mm of

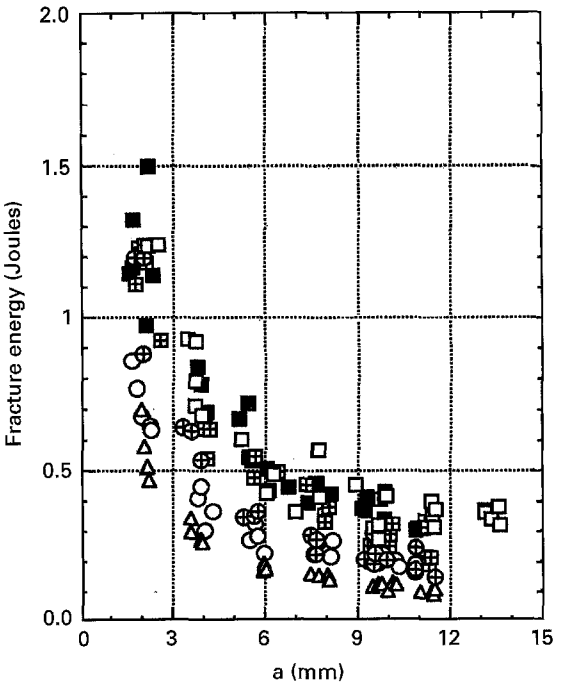

Figure 15 Fracture energy for SENT specimens versus crack length measured in the flow direction (MD) for the virgin material (□) and the reprocessed material after; ⊕ 1st, △ 2nd, ○ 3rd, ⊞ 4th and ■ 5th cycles.

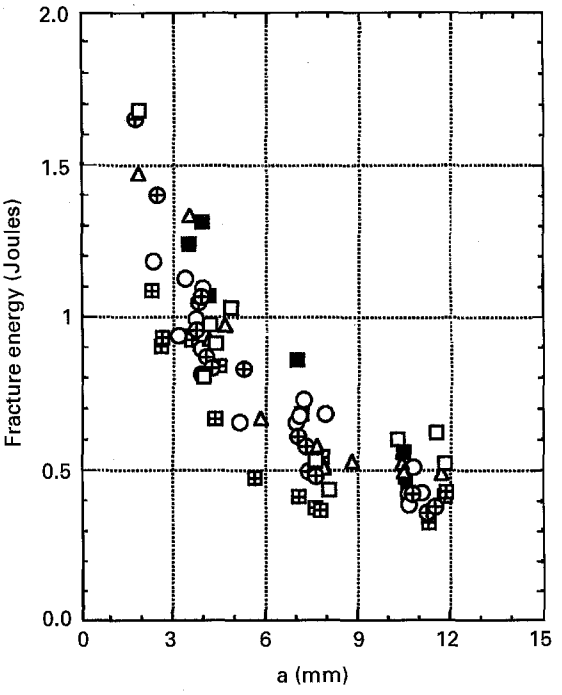

Figure 16 Fracture energy for SENT specimens versus crack length measured in the transverse direction (TD) for the virgin material (□) and the reprocessed material after; ⊕ 1st, △ 2nd, ○ 3rd, ⊞ 4th and ■ 5th cycles.

damage and stable crack growth would indeed be arbitrary. In point of fact, several tests were performed in which specimens were unloaded just before the maximum load was reached and the length of the damage zone and the stable crack growth, were then measured. It was found that although the length of the damage zone corresponding to maximum load did not vary significantly with varying a/D ratio it was nevertheless as large as 6–8 mm with a crack growth of about 1 mm. In view of this observation, the use of the 5% P_q approach would indeed be arbitrary. Nevertheless, when this procedure was applied, it was noted that for 90% of the data, P_q values were in close proximity to P_{max} (the ratio being less than 1.15) and as a result the calculated K_q values for valid test records did not differ significantly from the corresponding K_c values (see Fig. 11(a)).

Regarding the second question, in order to take into account the presence of the damage zone, the crack length, a, in Equation (2) was replaced by a fictitious crack length, c, defined as:

$$c = a + \frac{1}{2\pi}\left(\frac{K_c}{\sigma_y}\right)^2 \tag{4}$$

Equations (2), (3) and (4) were then iterated to determine c and to recalculate K_c. This procedure gave K_c values which were exceptionally high and consequently was not considered further.

Finally, implementing the ASTM specimen size criterion for valid plane–strain fracture toughness determination [4]

$$B \geq 2.5\left(\frac{K_c}{\sigma_y}\right)^2 \tag{5}$$

and using the average K_c value of 4 MPa m$^{1/2}$ and tensile yield stress value of 52 MPa, one observes that the minimum thickness requirement is approximately 15 mm which is considerably higher than the thickness used in this study. In view of this, the measured values are considered as "apparent fracture toughnesses" and as such they may vary with dimensions of the specimens. Nevertheless, they have been found to be useful for studying the effect of recycling on fracture toughness.

Figures 15 and 16 show the variation of energy required for fracture, U_f, (measured from the area under the load–displacement traces up to the point of maximum load) with crack length for the virgin and some selected reprocessed materials for both MD and TD directions respectively. Evidently, U_f, decreases with increasing crack length showing no systematic variation with the number of reprocessing cycles.

3.10. Fracture of the specimens with weld-lines

The fracture toughness of the specimens with weld-line was determined using single-edge notched specimens with the edge notch placed inside the weld-line and then applying the load normal to this line (i.e. as in TD specimens).

In order to examine the uniformity of the weld-line, specimens were cut from the plaque mouldings at three positions along the weld-line (i.e. P2, P4 and P6 as shown in Fig. 10). Fig. 17(a, b) shows typical plots of σ_f versus $[Ya^{1/2}]^{-1}$ for the condition in which the plaques were produced by two melt flow fronts advancing adjacently. From these plots the following observations can be made. In the first place, the variation of σ_f with $[Ya^{1/2}]^{-1}$ is linear indicating that

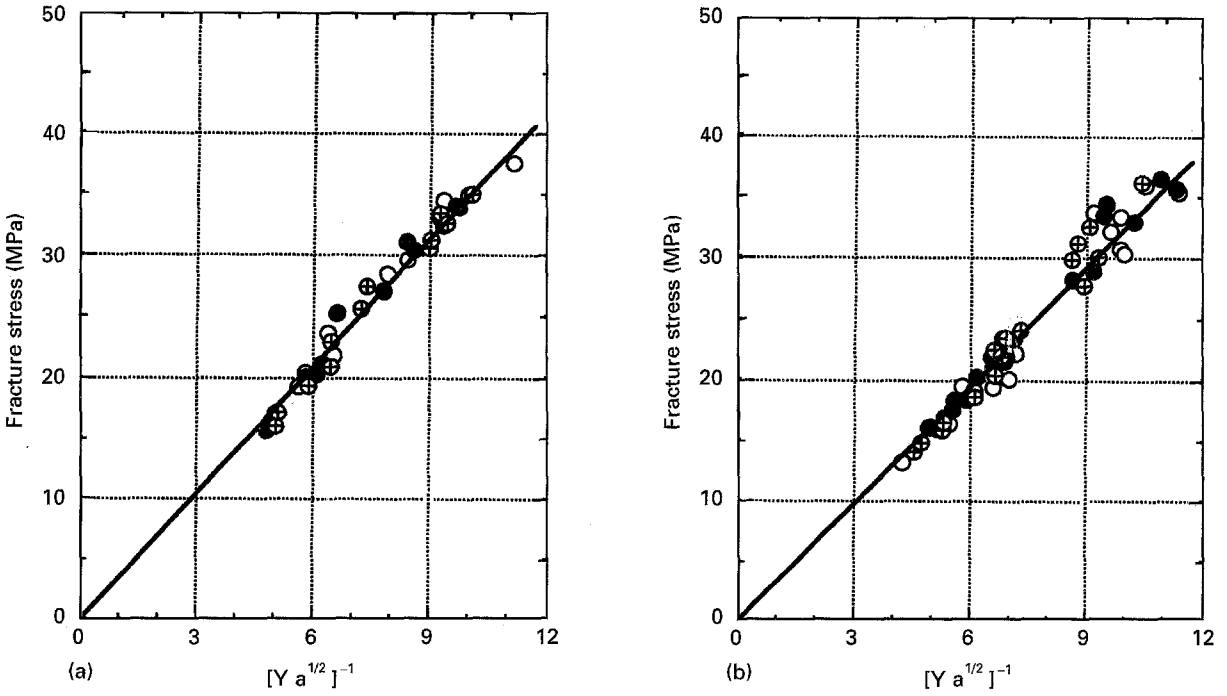

Figure 17 Fracture stress for SENT specimens with a weld-line versus $[Ya^{1/2}]^{-1}$ for (a) the virgin and (b) the fourth reprocessed material; ⊕ = P2, ● = P4 and ○ = P6.

LEFM can be used to determine fracture toughness from the welded specimens. In the second place, fracture toughness is not affected by the specimen position. Table V compares fracture toughness of the weld and weld free specimens. It can be seen that although fracture toughness is not affected significantly by the number of reprocessing cycles, it shows a clear reduction in the presence of a weld-line. The weld-line integrity factor defined as the ratio of the two toughness values indicates that K_c is affected significantly by the weld-line; giving a weld-line integrity factor of about 0.74. This reduction in toughness in the presence of the weld-line is attributed to the alignment of the fibres parallel to the weld-line and therefore transverse to the direction of the applied stress.

The influence of weld-line formed by two opposing flow fronts on fracture toughness is also evident from the data given in Table V. The reduction in fracture toughness may once again be attributed to the presence of the weld-line. However, values obtained from these specimens show a greater variation with the number of reprocessing cycles. It should be appreciated that an assessment based upon a direct comparison between the two weld-lines, that is, one formed by two opposing flow fronts and the other by two parallel flow fronts, would be invalid in our case due to the differences in specimen dimensions.

TABLE V Fracture toughness, K_c, for welded specimens [MPa $m^{1/2}$]

N_r	K_c, weld(1)	K_c, unwelded	F	K_c, weld(2)
0	3.51 ± 0.12	4.90 ± 0.16	0.72	3.85 ± 0.24
1	3.59 ± 0.09	4.82 ± 0.06	0.74	3.46 ± 0.24
2	3.57 ± 0.17	4.69 ± 0.12	0.76	3.28 ± 0.24
3	3.48 ± 0.18	4.60 ± 0.15	0.76	2.84 ± 0.24
4	3.31 ± 0.10	4.50 ± 0.17	0.74	2.54 ± 0.25
5	3.43 ± 0.11	4.62 ± 0.25	0.74	2.25 ± 0.22

Note: (*1*) adjacing flow fronts, (*2*) opposing flow fronts.

3.11. Flexural testing of notched bars

The fracture toughness of the virgin and the reprocessed materials was also measured in flexure using single-edge notched bend specimens (SENB) with span to depth ratio of 8:1 (see Fig. 10). The calibration factor Y used for this geometry is given by [4]:

$$Y = 1.96 - 2.75x + 13.66x^2 - 23.98x^3 + 25.22x^4 \quad (6)$$

The load–displacement traces obtained from these specimens had similar characteristics to those obtained for SENT, i.e. they exhibited some non-linearity before reaching the maximum load due to a small amount of crack extension and damage at the crack tip. The extent to which the damage zone propagated in these specimens was less than that produced in tension due to the compressive nature of the stress field in the specimens. The ratio of $P_{max}/P_{5\%}$ was less than 1.15 for the majority of test specimens and the plots of σ_f versus $[Ya^{1/2}]^{-1}$ as shown in Fig. 18(a–d) were essentially linear for a/D ratios greater than 0.1. Table VI gives fracture toughness (average ± 95% confidence limit) for the virgin and the reprocessed materials. In view of these results, it can be said that: K_c, decreases with the number of reprocessing cycles, with the virgin material giving 30% higher fracture toughness than the fifth reprocessed material. Comparison of SENT (MD specimens) and SENB results also indicate that the measured K_c value in bending is consistently higher than that measured in tension, for the same crack orientation. It is noteworthy that the unnotched flexural strengths were also consistently higher than tensile strengths. Thus

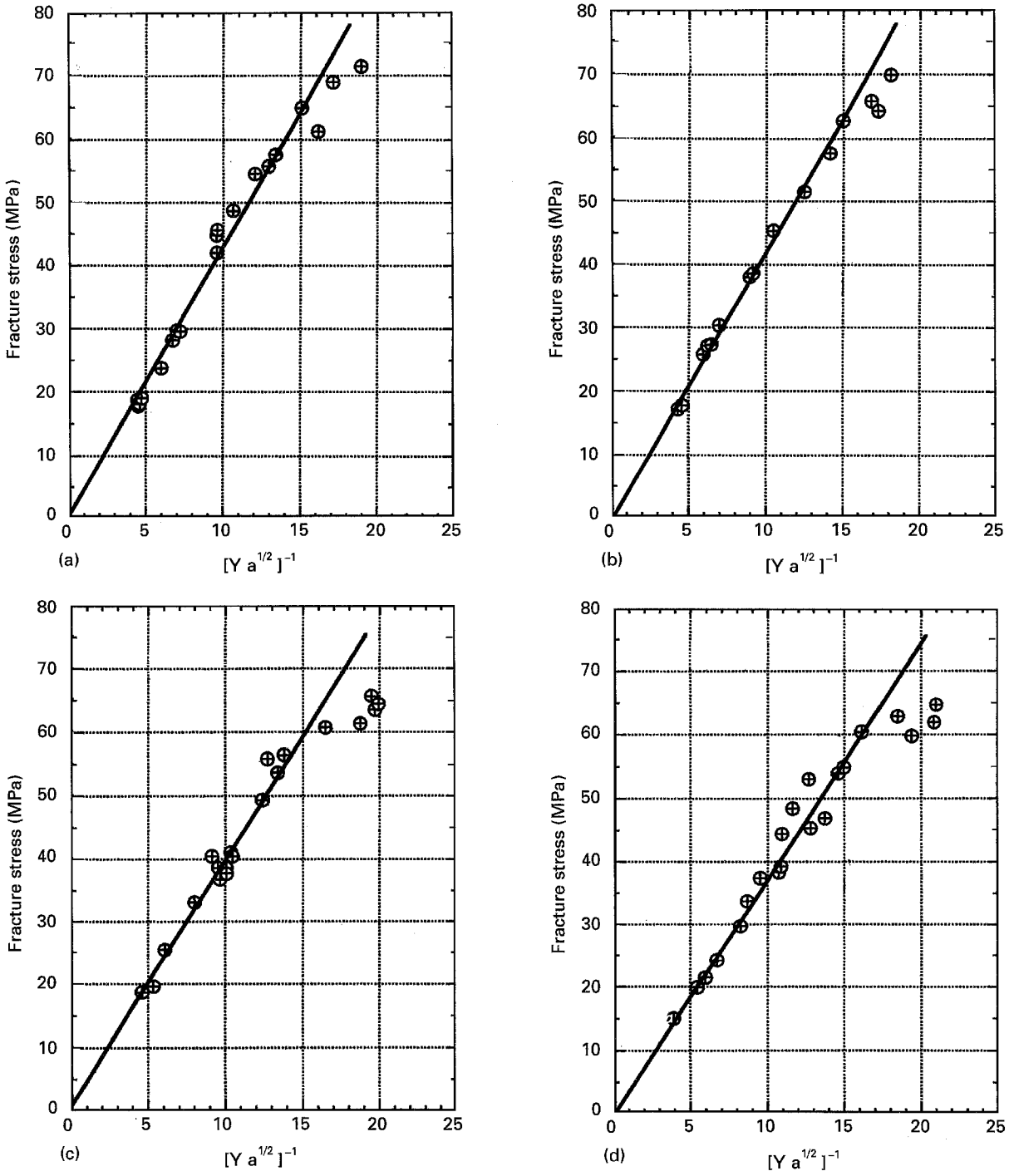

Figure 18 Fracture stress for SENB specimens versus $[Ya^{1/2}]^{-1}$ for (a) the virgin material and (b–d) the reprocessed material after 1, 3 and 5 cycles respectively.

TABLE VI Notched flexural data

N_r	K_c [MPa m$^{1/2}$]	G_c [kJ m^{-2}]	E^* [GPa]
0	4.38 ± 0.11	6.83 ± 0.44	2.81
1	4.23 ± 0.07	6.82 ± 0.63	2.62
3	4.00 ± 0.12	6.82 ± 0.31	2.35
4	3.85 ± 0.13	6.10 ± 0.65	2.43
5	3.75 ± 0.12	6.23 ± 0.48	2.26

suggesting that the differences in quantities for the two loading configurations is mainly due to the skin–core morphology which is expected to be different for the two mouldings (i.e. plaque mouldings versus flexural bars).

The strain energy release rate, G_c, was also calculated from the energy absorbed by the specimen up to the maximum load according to the following expressions [6]:

$$U_f = BD\phi G_c \tag{7}$$

where ϕ is a geometrical factor defined as:

$$\phi = \frac{C}{dC/d(a/D)} \tag{8}$$

where C is the compliance of the cracked sample. Tabulated values of ϕ as a function of a/D have already been given in reference [6]. Fig. 19(a–d), shows the variation of U_f with $BD\phi$ for the virgin and

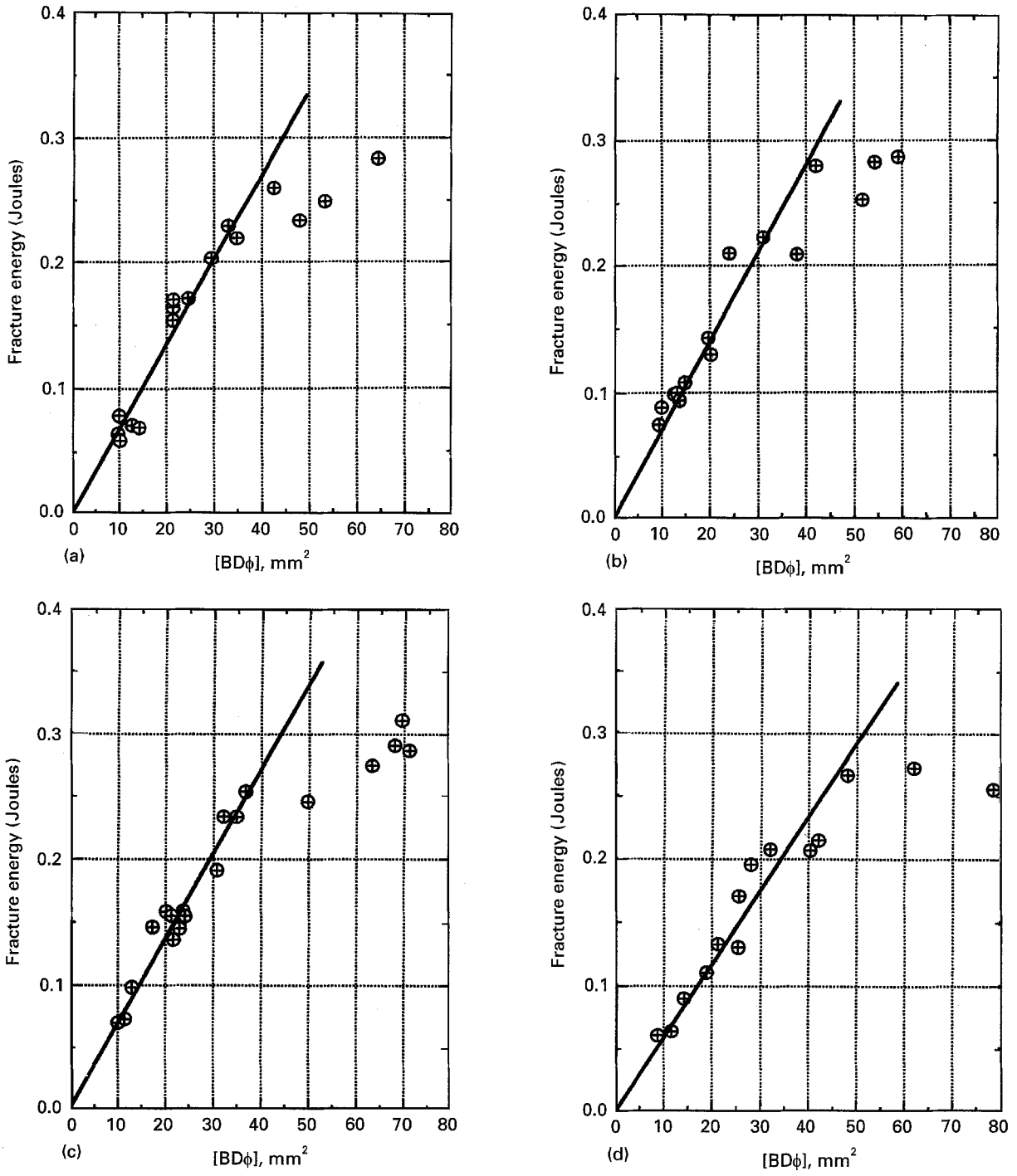

Figure 19 Fracture energy for SENB specimens versus BDϕ for (a) the virgin material and (b–d) the reprocessed material after 1, 3, and 5 cycles respectively.

three reprocessed materials is linear. Evidently, U_f varies linearly with $BD\phi$ over the range of a/D for which K_c is independent of crack length. Thus, enabling G_c to be determined from the slopes drawn in the Fig. 19(a–d). G_c values are delineated in Table VI and show very little variation with the number of reprocessing cycles.

The strain energy release rate is related to fracture toughness by the expression:

$$G_c = \frac{K_c^2}{E^*} \tag{9}$$

where E^* is the effective modulus. Using the G_c and K_c values given in Table VI, the effective modulus for each material was calculated via Equation 9. Clearly, the effective modulus is lower than that of flexural modulus and shows some variation with the number of reprocessing cycles. It must be noted, that the tip of crack in notched flexural bars, lies within the core region where fibre orientation is expected to be different to that of the skin layer, where the alignment is predominately in the flow direction of the polymer melt.

4. Conclusions

The influence of reprocessing by injection moulding on properties of polycarbonate has been studied. It was found that the number of reprocessing cycles:

(i) reduces the mean fibre length,

(ii) does not affect the infrared spectra, hence has no influence upon the chemical structure of the polymer,

(iii) increases the melt flow index due to the reduction in polymeric chain length as a result of degradation,

(iv) does not affect the tensile and flexural yield strengths nor does it affect the modulus of the material,

(v) reduces the impact strength of the material,

(vi) reduces the fracture toughness of the material particularly in the bending mode, where the damage zone at the tip of the crack is suppressed by the compressive stress field in the specimen,

(vii) does not affect strain energy release rate, G_c,

(viii) does not affect the tensile strength or fracture toughness of the material in the presence of the weld-line. This latter quantity does suffer considerably by the weld-line giving a weld-line integrity factor, F, of 0.75. The value of F was not affected significantly by the number of reprocessing cycles.

Acknowledgement

The authors wish to thank BAYER UK for the provision of the materials and Dr. A. Farid for his constructive criticisms.

References

1. J. I. EGUIAZABAL and J. NAZABAL, *Eur. Polymer.* **14** (1989) 891.
2. K. B. ABBAS, *Polym. Eng. Sci.* **20** (1980) 376.
3. *Idem., Polymer* **22** (1981) 836.
4. W. F. BROWN and J. E. SRAWLEY, ASTM STP 410 (1966).
5. D. O. HARRIS, *J. Bas. Eng.* **49** (1967) 89.
6. E. PLATI and J. G. WILLIAMS, *Polym. Eng. Sci.* **15** (1975) 470.

Received 4 April 1995
and accepted 8 September 1995